X-Ray Scattering Measurements of Radiative Heating and Cooling Dynamics

G. Gregori

Lawrence Livermore National Laboratory, University of California, P.O. Box 808, California 94551, USA
Clarendon Laboratory, University of Oxford, OX1 3PU, United Kingdom

S. H. Glenzer, K. B. Fournier, K. M. Campbell, E. L. Dewald, O. S. Jones, J. H. Hammer, S. B. Hansen, R. J. Wallace, and O. L. Landen

Lawrence Livermore National Laboratory, University of California, P.O. Box 808, California 94551, USA
(Received 4 November 2005; published 24 July 2008)

Spectrally and time-resolved x-ray scattering is used to extract the temperature and charge state evolution in a near solid density carbon foam driven by a supersonic soft x-ray heat wave. The measurements show a rapid heating of the foam material ($\sim$200 eV/ns) followed by a similarly fast decline in the electron temperature as the foam cools. The results are compared to an analytic power balance model and to results from radiation-hydrodynamics simulations. Finally, the combination of charge state and temperature extracted from this known density isochorically heated plasma is used to distinguish between dense plasma ionization balance models.

DOI: 10.1103/PhysRevLett.101.045003 PACS numbers: 52.25.Os, 52.40.Db, 52.50.Jm, 52.70.La

The radiative heating of low atomic number matter by soft x rays plays a central role in indirect-drive inertial confinement fusion (ICF) [1], high energy density science [2,3], and stellar and interstellar environments [4]. In particular, for a given radiation source, the radiative ablation rate [5] and burnthrough will be determined by the opacity and heat capacity of the heated material, which, in turn, is dependent on the electron temperature T_e and ionization state Z reached. In indirect-drive ICF, the hydrodynamic efficiency of CH capsule ablators [6] depends on the soft x-ray opacity and, in particular, the number of remaining bound carbon K-shell electrons at $T_e = 200$–300 eV. At lower densities or higher radiation temperatures, the radiation field switches from driving subsonic ablation to driving a supersonic ionization wave [2,3,7]. Such supersonically heated low atomic number plasmas are an integral part of heavy ion beam fusion target designs [8] that use the plasma thermal pressure $\sim Zn_iT_e$ as well as ablation pressure to drive high atomic number payloads [2]. Since the Rosseland mean opacity of the heated low atomic number material is at times <1 [2], nonlocal thermodynamic equilibrium (non-LTE) between the material and the radiation must be assumed, and this would benefit from independent measurement of the parameters T_e and Z that determine the thermal pressure. Both heating and cooling phases are of interest since the low atomic number thermal pressure n_eT_e can be made to dominate over the high atomic number payload ablation pressure [1,9] by allowing the radiation drive to drop in time or turn off.

Traditionally, the conditions in radiatively heated low atomic number dense matter have been determined by either line absorption spectroscopy or inferrence from soft x-ray burnthrough measurements. Optical Thomson scattering which has been successfully applied at low density [10] to extract T_e and Z is limited to electron densities below 10^{21} cm^{-3}. Line emission spectroscopy at perforce sub-keV photon energies suffers from low contrast due to large line center optical depths and strong sensitivity to non-LTE effects and high energy radiation components. Line absorption spectroscopy is also limited to the sub-keV region and very thin samples (e.g., Ref. [11]) or uses midatomic number tracer layers such as Mg, Al, Cl, and Ti for which the K-shell absorption spectra are above 1 keV. Soft x-ray burnthrough measurements are more indirect and must be compared to radiation-hydrodynamics modeling to infer material conditions (see, e.g., Ref. [12]).

In this Letter, we demonstrate an alternate technique: multi-keV spectrally resolved x-ray scattering [13] for a noninvasive simultaneous time-resolved measurement of temperature and ionization state of radiatively heated carbon foam samples. The x-ray scattering technique in the noncollective regime provides a direct measurement of the electron distribution function and, consequently, a measurement of the electron temperature which does not rely on a specific plasma model [14]. Under noncollective scattering, the probe scale length [defined in terms of the scattering wave number $k = 4\pi E_0 \sin(\theta/2)/hc$, where E_0 is the probe energy, h the Planck constant, c the speed of light, and θ the scattering angle] is much smaller than the characteristic interparticle correlation distance (given by the Debye length λ_D), and thus $k\lambda_D \gg 1$ [15].

The experimental setup is illustrated in Fig. 1. A 0.2 g/cm^3, 900 μm diameter, and 300 μm thick carbon foam (93% C, 6% O, and 1% H by weight) is placed on one end of a 1.2 mm long, 1.2 mm diameter gold hohlraum with a 600 μm diameter laser entrance hole (LEH). The hohlraum is driven with 13 (18) frequency tripled (3ω, 351 nm) beams of the Omega facility [16] yielding 6.2 (8.5) kJ in 1 ns to produce a relatively uniform soft x-ray radiation bath inside the gold cavity. During the duration of the experiment, the near blackbody radiation flux, defined for

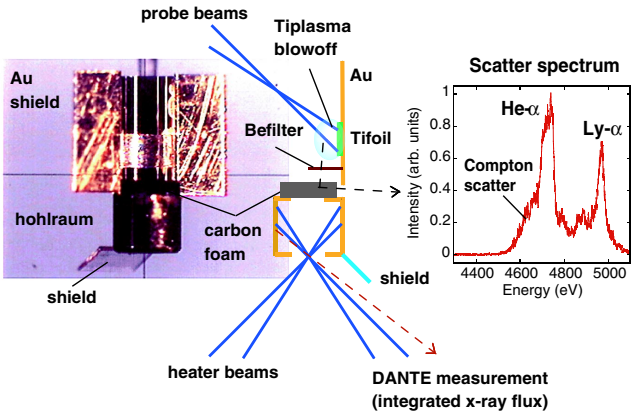

FIG. 1 (color online). Schematic of the experimental setup, showing the carbon foam payload driven by the hohlraum radiation field. On the right side, a measured spectrum is reported. Notice a weaker Ly-α on the high energy side of the He-α.

emission below 2 keV, emitted by the hohlraum, is measured with DANTE, an absolutely calibrated diode array x-ray flux detector, providing a time-dependent radiation temperature T_R. In order to measure the supersonic ionization wave driven by the hohlraum into the foam, near the end of the driving laser beams, a second set of 10 ns long beams (4.7 kJ) is fired onto a Ti foil (see Fig. 1) to produce the 4.75 keV He-α probe line. The Ti He-α scattered by the foam at $\theta = 95^{\circ}$ is spectrally resolved with a high efficiency graphite Bragg crystal with spectral resolution $\Delta E/E \sim 6 \times 10^{-3}$ [13] and temporally resolved with an x-ray framing camera. A thin (100 μm thick) Be foil is placed between the carbon foam and the Ti foil in order to prevent the Ti plasma blowoff from entering into the line of sight, defined by a 250 μm wide slit towards the direction of the spectrometer. The Be filter has >90% transmission at 4.75 keV and at the same time blocks soft x rays from the Ti plasma heating the foam.

Experimental scattering spectra obtained at $t = 0.7$, 1.1, and 1.5 ns (where $t = 0$ corresponds to the start of the drive beams) are given in Fig. 2 for the case of the 8.5 kJ drive beams. The inferred presence of Ly-α emission indicates that Li-like satellites do not make a significant contribution to the He-α spectrum. We see that the experimental data show a primary line at the frequency of the x-ray probe (which corresponds to elastically scattered photons) and a redshifted wing resulting from Compton scattered photons that have lost a fraction of their initial energy as they collide with free electrons in the foam plasma. The intensity of this inelastic component gets more pronounced just after the end of the hohlraum drive (at 1.1 ns), suggesting a larger degree of ionization in the plasma. Similarly, at $t =$ 1.1 ns the inelastic redshifted component is also considerably broadened when compared to the other two measured times. As discussed in Refs. [13,14,17], the width of the inelastic component is proportional to $T_e^{1/2}$, and this shows at $t = 1.1$ ns a significantly hotter plasma. The intensity

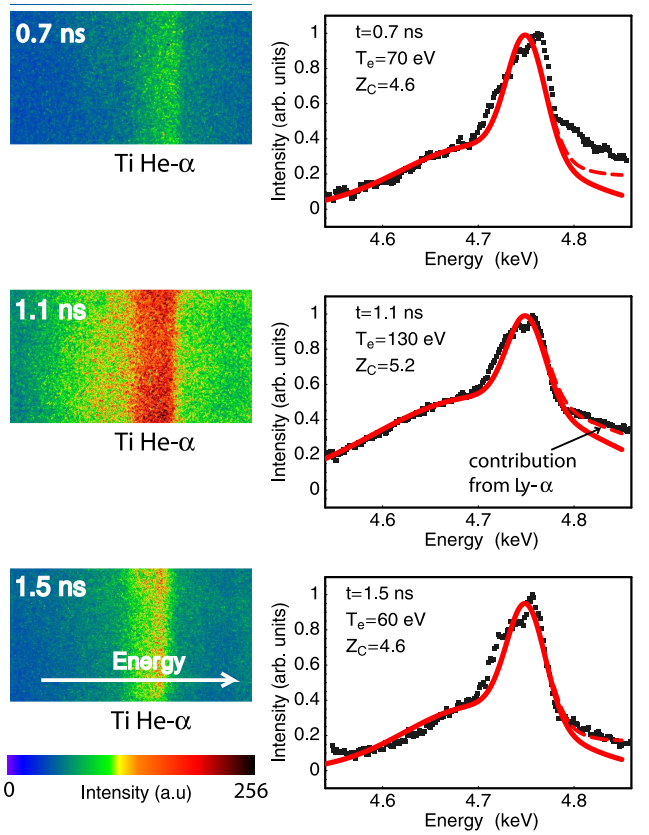

FIG. 2 (color online). Experimental x-ray framing images of the scattered Ti He-α line (left column). The corresponding lineouts obtained by summing the pixel counts over the non-dispersive direction are reported in the right column together with best fit values for T_e and Z_C. All of the spectra have been normalized to peak intensity equal to 1. The theoretical spectra have been convolved with the instrument function inferred from the measurement of the Ti He-α source spectrum, as discussed in Ref. [13]. The dashed lines correspond to spectra calculated including the contribution of the Ti Ly-α line at 4.99 keV.

ratio between the elastic to the inelastic features is $\sim Z_b^2/Z_f$ (where Z_b is the number of bound electrons and Z_f the number of free electrons), which allows a direct measurement of the ionization state. In order to obtain accurate electron temperatures and electron densities in the foam, the experimental spectra have been fitted with a multicomponent scattering form factor [17,18] which includes all of the relevant scattering processes from bound and free electrons as well as relativistically correct wave functions (important for the inner shell bound electrons) and partial degeneracy (necessary at high electron densities). Best fits of the experimental spectra are also reported in Fig. 2 together with the corresponding values for T_e and the carbon ionization Z_C. In the model, it is assumed that the hydrogen in the foam is fully ionized ($Z_H = 1$) and the oxygen has an average ionization $Z_O = 6$, which is expected from the Thomas-Fermi model at $T_e \sim 100$ eV [19]. While this is an approximation and errors are expected in Z_O (and possibly Z_H), Z_C remains rather insen-

sitive on the exact values for the hydrogen and oxygen ionization, due to their small concentration in the foam. In addition, fractional values for the carbon ionization are inferred by considering a weighted distribution of only the two nearest ionization states. As discussed in Ref. [18], the error introduced by such an approximation can be estimated as ~20%.

The measured values for T_e in the foam for both the 8.5 and the 6.2 kJ drives are reported in Fig. 3 together with the measured blackbody radiation flux inside the hohlraum (T_R) obtained from DANTE. A simple analytical model that relates the drive flux incident on the foam with the foam temperature can be derived. Neglecting transmission through the foam, and ignoring cross coupling with the hohlraum radiation field, power conservation requires that the incident radiation flux (S_i) on the foam must be balanced by absorption ($S_{\rm abs}$), reemission (S_r), and convection ($S_{\rm conv}$), i.e., $S_i = S_{\rm abs} + S_r + S_{\rm conv}$. Assuming that the foam is reradiating in LTE (because we are near solid density), we have [20]

$$S_i = A_i \sigma T_R^4, \qquad S_{\rm abs} = A_i \frac{d(\epsilon_{\rm th} x)}{dt}, \qquad S_r = A_f \sigma T_e^4,$$
$$S_{\rm conv} = 3 A_f Z n_i k_B T_e c_s, \tag{1}$$

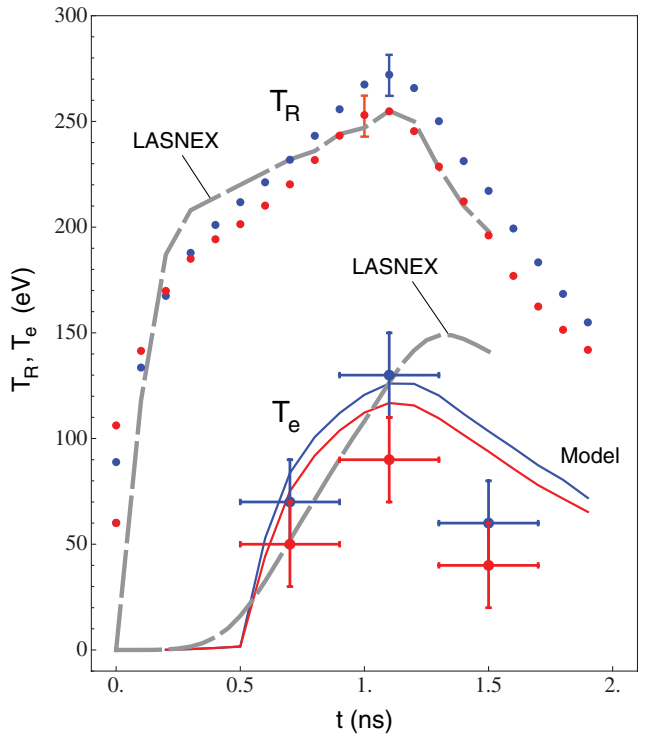

FIG. 3 (color online). Time evolution of the radiation temperature in the hohlraum (T_R) measured by DANTE (solid points). The electron temperature (T_e) in the foam is given: experimental data versus scaling derived from analytical power balance (solid lines). Blue: 8.5 kJ laser drive; red: 6.2 kJ laser drive. LASNEX calculations assuming 8 kJ of laser energy coupled into the hohlraum are also reported (dashed lines).

where $A_i = \pi R_i^2$ is the area of the foam exposed to the hohlraum flux, A_f is the foam surface area (which includes thermal expansion), σ is the Stefan-Boltzmann constant, k_B is the Boltzmann constant, $\epsilon_{\rm th}$ is the thermal energy density in the foam, $c_s = \sqrt{Z k_B T_e / M}$ is the sound speed, with M the carbon mass, and x is the penetration depth of the radiation front. The ion density $n_i = \rho \mathcal{N}_{av}/A$ is assumed to remain approximately constant ($\rho = \rho_0 = 0.2$ g/cm^3) for the current supersonic heat wave conditions proven later (i.e., no shock forms). We can approximate

$$\epsilon_{\rm th} \approx \frac{3}{2} Z n_i k_B T_e = \frac{3\sqrt{3}\mathcal{N}_{av}\rho_0}{2A\sqrt{I_H}} (k_B T_e)^{1.5}, \tag{2}$$

with $\mathcal{N}_{\rm av}$ the Avogadro number, A the atomic weight of carbon, and I_H the ionization energy of the hydrogen atom. In Eq. (2), we have used the relation $Z^2 I_H \sim 3 k_B T_e$. We should note that in obtaining $\epsilon_{\rm th}$ we have neglected contribution from the ion thermal energy as well as ionization energies. This introduces a correction of $\lesssim 20\%$ for partially ionized carbon atoms $Z \lesssim 4$–5. The foam surface area is approximated as

$$A_f(t) = \pi[1 + U(x)]R_f^2 + 2\pi R_f (x + c_s t), \tag{3}$$

where $U(x) = 0$ if $x < L_f$ and $U(x) = 1$ otherwise, with R_f the foam radius and L_f its thickness. The first part on the right-hand side of Eq. (3) accounts for the fact that, until the radiation wave has burnthrough, reemission of the radiation is important only towards the hohlraum side. The second part of Eq. (3) includes the change in the lateral surface area due to expansion. The penetration depth in the diffusive approximation relevant here is given by $x = \min(L_f, t^{0.5} T_e^2/\sqrt{\kappa})$ and $\kappa = 0.3\epsilon_{\rm th}/\sigma\lambda_R$ [3], with a calculated $\lambda_R(\mu{\rm m}) = 0.12[T_e({\rm eV})]^2$ [21]. Since the time-dependent incident flux T_R is known from DANTE, the power balance can be solved numerically for T_e and x. We calculate a burnthrough time (when $x = L_f$) of ~0.7 ns, consistent with simulations (see below), also validating the supersonic flow approximation (i.e., $dx/dt = 430$ μm/ns is bigger than $c_s = 75$ μm/ns).

Temperature profiles in the foam and inside the hohlraum have also been obtained using LASNEX [22], which includes both non-LTE effects, radiative transport, hydrodynamics, and warm opacities, as well as full coupling of the laser light into the hohlraum. LASNEX models the measured T_R exiting the LEH relatively well at all times. During the heating phase, LASNEX T_e results are in good agreement with the experimental data, showing a fast delayed rise in the electron temperature (~200 eV/ns). The fast measured foam cooling after the laser drive is off is unexpected and merits further measurements using a more collimated probe to avoid being dominated by the physics of edge regions adiabatically cooling either by rarefaction or by conduction to colder Au walls.

In Fig. 4, calculated values from two codes for the average ionization of carbon at 0.2 g/cm^3 as a function

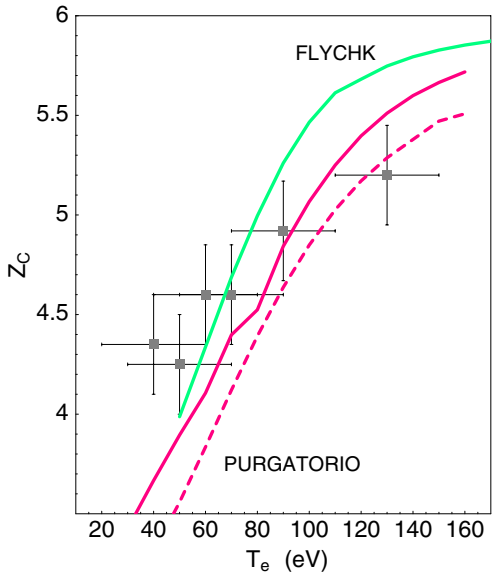

FIG. 4 (color online). Ionization balance plot for the 0.2 g/cc foam. The experimental data are compared with PURGATORIO and FLYCHK. Two PURGATORIO values are given: one including all continuum electrons (solid line) and one which excludes continuum electrons in quasibound resonance states (dashed line).

of temperature are compared with the benchmark ionization and temperature measurements. FLYCHK [23,24], a non-LTE collisional-radiative code using atomic data constructed in the hydrogenic approximation and including the effects of continuum lowering, gives calculated values that agree well with the measurements for $T_e \lesssim 100$ eV. The other code, PURGATORIO [25], is a new implementation of the INFERNO [26] algorithm for equation-of-state (EOS) calculations. It provides a fully relativistic, quantum mechanical description of an average atom embedded in a uniform plasma. The quantum mechanical treatment of continuum electrons allows PURGATORIO to follow the evolution of bound states as they dissolve under pressure ionization to form resonance (quasibound) features in the continuum density of states, ensuring continuity and overcoming a fundamental defect of EOS models which treat continuum electrons in the Thomas-Fermi approximation (such as those used to generate the EOS data used in the present LASNEX calculations). Since the present x-ray scattering measurements treat free and quasibound electrons on the same theoretical ground within the random phase approximation [17], they are especially useful as benchmarks for total ionization, and the solid line in Fig. 4 giving the total continuum charge calculated using PURGATORIO agrees reasonably well with the measurements over the entire temperature range.

In conclusion, in this Letter we have demonstrated that multi-keV spectrally and time-resolved x-ray scattering can be successfully implemented as a noninvasive diagnostics of electron temperature and ionization state in radiatively driven foams. The simultaneous measurement of both the radiation temperature in the hohlraum and the electron temperature in the foam allows a direct validation of near solid density plasma models. Our results are important for the understanding of the energy deposition and transport in radiation-driven ablation processes of high density matter, which is relevant for the success of ICF.

The authors thank B. Wilson, V. Sonnad, P. Sterne, and W. Isaacs for allowing us to use the PURGATORIO code. This work was performed under the auspices of the U.S. Department of Energy by the University of California Lawrence Livermore National Laboratory under Contract No. W-7405-ENG-48. We also acknowledge support from Laboratory Directed Research and Development Grant No. 05-ERI-003. The work of G. G. was partially supported by the Science and Technology Facilities Council of the United Kingdom.

[1] J. D. Lindl, *Inertial Confinement Fusion* (Springer-Verlag, New York, 1998).
[2] M. J. Edwards *et al.*, Phys. Plasmas **7**, 2099 (2000).
[3] C. A. Back *et al.*, Phys. Rev. Lett. **84**, 274 (2000).
[4] D. Mihalas and B. W. Mihalas, *Foundation of Radiation Hydrodynamics* (Oxford University Press, New York, 1984).
[5] R. E. Marshak, Phys. Fluids **1**, 24 (1958).
[6] N. Kaiser *et al.*, Phys. Fluids **1**, 1747 (1988).
[7] J. Massen *et al.*, Phys. Rev. E **50**, 5130 (1994).
[8] D. A. Callahan and M. Tabak, Nucl. Fusion **39**, 883 (1999).
[9] M. D. Rosen, Phys. Plasmas **3**, 1803 (1996).
[10] S. H. Glenzer *et al.*, Phys. Rev. Lett. **82**, 97 (1999).
[11] B. A. Hammel *et al.*, Europhys. Lett. **20**, 319 (1992).
[12] R. E. Olson *et al.*, Phys. Plasmas **11**, 2778 (2004).
[13] S. H. Glenzer, Phys. Rev. Lett. **90**, 175002 (2003).
[14] O. L. Landen, J. Quant. Spectrosc. Radiat. Transfer **71**, 465 (2001).
[15] J. Sheffield, *Plasma Scattering of Electromagnetic Radiation* (Academic, New York, 1975).
[16] J. M. Soures *et al.*, Fusion Technol. **30**, 492 (1996).
[17] G. Gregori *et al.*, Phys. Rev. E **67**, 026412 (2003).
[18] G. Gregori *et al.*, J. Quant. Spectrosc. Radiat. Transfer **99**, 225 (2006).
[19] D. Salzmann, *Atomic Processes in Hot Plasmas* (Oxford University Press, Oxford, England, 1998).
[20] R. Siegel, in *Laser Plasma Interactions 5: Inertial Confinement Fusion*, edited by M. B. Hooper and P. Osborne (Institute of Physics Publishing, Bristol, England, 1995).
[21] R. P. Drake, *High Energy Density Physics* (Springer, Berlin, 2006).
[22] G. B. Zimmerman and W. L. Kruer, Comments Plasma Phys. Control. Fusion **2**, 51 (1975).
[23] H.-K. Chung *et al.*, J. Quant. Spectrosc. Radiat. Transfer **81**, 107 (2003).
[24] R. W. Lee and J. T. Larsen, J. Quant. Spectrosc. Radiat. Transfer **56**, 535 (1996).
[25] B. Wilson *et al.*, J. Quant. Spectrosc. Radiat. Transfer **99**, 658 (2006).
[26] D. A. Lieberman, Phys. Rev. B **20**, 4981 (1979).